Journal of Catalysis 422 (2023) 1–11

Contents lists available at ScienceDirect

Journal of Catalysis

journal homepage: www.elsevier.com/locate/jcat

CO_2 electroreduction on single atom catalysts: Is water just a solvent?

Debolina Misra [a,b], Giovanni Di Liberto [b], Gianfranco Pacchioni [b,*]

[a] Department of Physics, Indian Institute of Information Technology, Design and Manufacturing, Kancheepuram, Chennai 600127, India
[b] Dipartimento di Scienza dei Materiali, Università di Milano – Bicocca, via R. Cozzi 55, 20125 Milano, Italy

ARTICLE INFO

Article history:
Received 18 February 2023
Revised 24 March 2023
Accepted 2 April 2023
Available online 5 April 2023

Keywords:
CO_2 reduction
Electrocatalysis
DFT calculations
Solvent effects
Reaction intermediates

ABSTRACT

The electrochemical reduction of CO_2 on single atom catalysts (SAC) has emerged as a highly promising yet intricate process, requiring an in-depth understanding of each elementary step of the reaction. Most of the theoretical studies pertaining the screening of new efficient catalysts neglect important effects such as the capability of the catalytic site to bind and activate CO_2, the occurrence of competing reaction paths *via* formation of different isomers in the intermediate steps, and the role of water. In this work we will show that these are key aspects of the CO_2 reduction reaction (CO_2RR). Employing density functional theory, we investigated a series of Transition Metal atoms (Sc-Cu, Mo-Ag, W-Au) embedded in nitrogen doped graphene (TM@4N-Gr) and their activity in the CO_2 reduction. Our results show that water is not only solvating the reaction intermediates, but it acts as a ligand itself, competing with CO_2 when binding to the catalytic site. This coordination chemistry effect largely affects the stability of the chemical intermediates. Furthermore, only a small fraction of the investigated SACs can bind and activate CO_2, and that in most cases the reaction proceeds *via* formation of the OCHO intermediate and not of the COOH one, as often assumed.

1. Introduction

Electro-catalytic reduction of CO_2 into valuable fuels has emerged as a promising way to reduce the CO_2 content in the environment and also to address the current energy crisis [1–10]. Since the conventional catalysts suffer from poor selectivity and stability, high cost and low transformation efficiency, the design and development of new catalysts with better efficiency and stability becomes imperative [11,12]. In this regard, Single Atom Catalysts (SAC) [13–15] made by Transition Metals (TM) embedded in carbonaceous matrixes, such as nitrogen-doped graphene, have recently emerged as potential catalysts for the CO_2 reduction reaction (CO_2RR) [16–18]. While single metal atoms have already shown better activity than their bulk counterparts [14,19–24], anchoring them in N-doped Graphene (N-Gr) resulted in excellent stability and tenability [25], in addition to an enhanced activity [26–36]. Several experimental and theoretical studies on the catalytic activity of TM@N-Gr for CO_2RR have been reported. In this respect, it is crucial to clarify what is the new message that one wants to convey with another study on this class of catalysts.

In the following, we will analyse the role of water, an essential ingredient of the reaction in the liquid phase, showing that water does not only solvate the reaction intermediates, but can compete with the weakly bound CO_2 molecule, acting as a ligand to the catalytic active site. This result can be interpreted in the light of the reminiscences between SACs and coordination chemistry compounds [37–40]. In addition to the main message, we discuss a few aspects, often neglected, which are relevant for a credible prediction of the CO_2RR on 2D catalysts. CO_2 thermal or electroreduction is a complex process that can lead to various products, such as HCOOH, CH_3OH, CO, CH_4 and others. Furthermore, in water the process of reducing CO_2 competes with the hydrogen evolution reaction (HER), another factor that often limits efficiency. It is important to mention that our goal is not that to predict a potential new catalyst for the reaction, but rather to point to some critical aspects of the process that need to be properly considered in theoretical studies. For this reason, we will not study the entire sequence of reduction steps that, starting from CO_2, may lead to CH_4 as one of the final products. Rather, we will concentrate on the first two steps of the reaction, i.e., CO_2 binding and activation, and CO_2 reduction to COOH. As we will show below, this is sufficient to demonstrate the importance of a few aspects that are often neglected in the discussion of the activity of SACs in CO_2RR.

The first question that we will address is the adsorption of CO_2 on the catalyst surface. An efficient catalyst must activate the inert

* Corresponding author at: Università Milano-Bicocca, Dipartimento di Scienza dei Materiali, via R. Cozzi 55, 20126 Milano, Italy.
E-mail address: gianfranco.pacchioni@unimib.it (G. Pacchioni).

https://doi.org/10.1016/j.jcat.2023.04.002
0021-9517/

CO_2 molecule causing a significant distortion of the OCO bond angle. Formation of a sufficiently stable complex where CO_2 is activated is an essential prerequisite of an efficient electro-catalysts for CO_2RR. There is a substantial difference for a reaction occurring in gas-phase or in water: in the gas phase even a weakly adsorbed and activated species can lead to a catalytic reaction provided that the partial pressure of that specific reactant is large enough to move the equilibrium towards the products. But in water solution, as is the case of electrocatalytic reactions, it is much harder to play with this parameter. Thus, CO_2 activation becomes crucial.

Interestingly, in many theoretical studies of CO_2RR this is not considered an important step, and reaction profiles are computed also for catalysts where CO_2 does not bind, or binds very weakly, to the catalytic sites. We will show that only a small minority of the TM@4N-Gr catalysts considered are able to bind and activate CO_2, the rest being completely inert.

Next, we will consider the role of the formation of different isomers in the first step of CO_2 reduction. The formation of different intermediates results in completely different reaction mechanisms; also in this case, most of the reported screening studies concentrates only on one kind of intermediates, COOH, thus neglecting other important reaction paths [41–44]. Based on density functional theory (DFT), we studied 19 TMs anchored on nitrogen-doped graphene. We will show that CO_2 activation, stability of reaction intermediates, and interaction with water are three crucial factors that need to be taken into account in the theoretical screening of single atom electrocatalysts for CO_2RR.

We organized the article as follows: Section 2 provides the computational details. In Section 3.1. we discuss our results on the activation of CO_2 and the stability of the reaction intermediates on the catalyst surface neglecting the presence of water (gas-phase reactions). In Section 3.2, the role of water both as a solvent and as a ligand will be discussed in detail. The conclusions are summarized in Section 4.

2. Computational details

Spin-polarized DFT calculations as implemented in Vienna Ab Initio Simulation Package (VASP) [45,46], were performed employing the projector-augmented wave (PAW) method [47] and the valence electrons were expanded with a set of plane waves with a kinetic cutoff equal to 400 eV. The Perdew, Burke, and Ernzerhof (PBE) functional [48] within the generalized gradient approximation (GGA) was used in all our calculations; the Van der Waals interactions were described using the D3 Grimme's correction [49]. The reciprocal space was sampled in order to provide converges results [28]. A working 5 × 5 × 1 Monkhorst-Pack grid was adopted. The convergence criteria for the electronic and ionic loops were set at 10^{-6} eV and 10^{-3} eV/Å respectively.

We fully optimized a 4x4 supercell of graphene, $a = b = 9.87$ Å and $\gamma = 120°$. It was used to construct the 4 N-Gr support where a 15 Å vacuum was included along the z direction to avoid interaction between the periodic images. A C-divacancy was created in the cell, followed by replacement of 4C atoms by N atoms to build the 4N-Gr (pyridine) support. The TM atom was embedded in the coordination site resulting in the TM@4N-Gr structure [50–52]. In each case, the atomic coordinates have been fully relaxed. The approximation of keeping frozen the lattice vectors at those of graphene implies a negligible error, less than 0.1 eV [28], and therefore it can be considered acceptable given the purpose of the study.

The adsorption energy (ΔE_{ads}) of an adsorbed molecule on the TM@4N-Gr catalyst is calculated as

$$\Delta E_{ads} = E_{cat+mol} - E_{cat} - E_{mol} \quad (1)$$

Where $E_{cat+mol}$, E_{cat} and E_{mol} are the energies of the catalyst with the molecule adsorbed, of the bare catalyst and of the molecule respectively. To calculate the reaction free energy for each of the reaction steps, we followed Norskov's Computational Hydrogen Electrode (CHE) approach [53],

$$\Delta G = \Delta E_{ads} + \Delta_{ZPE} - T\Delta S \quad (2)$$

where ΔE_{ads} refers to the DFT reaction energy, Δ_{ZPE} and ΔS are the changes in zero-point energy and entropy, respectively. The values of ZPE and entropic contributions for CO_2, H_2O and the reaction intermediates are taken from the literature [18] and NIST database [54] respectively. The entropy of gas phase molecules was taken from the NIST database, and that of solid-state species were neglected [55]. A way to overcome this approximation is to estimate the vibrational entropy of solids by means of the partition function formalism and working in a harmonic fashion, a rather crude approximation with hydrogen-containing systems [56]. If one neglects this contribution the expected error is about 0.1–0.2 eV, which can be considered acceptable given the specific purpose of the study. It should be mentioned, however, that if one aims at reproducing the experimental complexity this effect should be accounted for, together with many other effects such as solvation, applied voltage and pH. Further details and working equations are reported in the SI.

An important aspect in the computational study of SACs is their stability. Besides being active and selective, SACs need to be stable under reaction conditions. There are various aspects to take into account, such as sintering resistance, mainly related to the energy barriers for the SAs to diffuse on the support, or the electrochemical stability that can be evaluated by calculating the dissolution potential of the SA defined as $U_{diss} = U_{diss}(bulk) - E_f/eN_e$, where $U_{diss}(bulk)$ and E_f are the standard dissolution potential and the Fermi level of the bulk metal, respectively, and N_e the number of electrons involved [57]. Finally, also the effect of pH and applied potential can be considered by constructing Pourbaix diagrams [58]. These aspects are essential in order to predict new potential catalysts for a given reaction. However, the purpose of this work is not the prediction of new catalysts but only to show the important role of CO_2 activation and water coordination in CO_2RR. Thus, the stability issue will not be further considered.

3. Results and discussion

3.1. CO_2 activation and reaction intermediates

3.1.1. CO_2 activation on bare catalyst (no solvent)

CO_2 activation is the first key step for CO_2RR, where the bending of the CO_2 molecule reflects the activation of the molecule. However, in most of the theoretical studies on this topic, activation of CO_2 over the catalyst surface is not discussed, and it is simply assumed that the reaction can proceed even in the presence of an extremely weakly bound linear CO_2 molecule. Thus, as a first step in our study we analysed the TM@4N-Gr SACs and their capability to activate CO_2 (see Table 1 for the binding energies of the CO_2 molecule (ΔE_{ads}), the free energy for CO_2 activation (ΔG), the geometry of the complex, and the TM atom magnetization). Among the TM atoms studied, only Sc, Ti, Mo, Ru, W and Os embedded in 4N-Gr activate the CO_2 molecule, Fig. 1. All the remaining systems, including Pt, Pd, and other active metals, are totally inert.

If the reaction occurs on a solid–gas interface, with no solvent involved, then it becomes unclear how it can proceed if the reactant (CO_2) binds very weakly to the catalyst, unless elevated CO_2 pressures are used. If reaction occurs in aqueous solution, then the effect of the solvent needs to be included (see Section 3.2).

For the SACs where CO_2 is spontaneously activated, Fig. 1, we observe various binding modes and binding strengths of the CO_2

Table 1
Binding properties of a CO_2 molecule on TM@4N-Gr: adsorption energy, adsorption free energy, O-C-O bond angle, C-O and TM—C distances, magnetization of TM and Bader charge on CO_2 for the CO_2RR in absence of solvent.

TM	ΔE_{ads} / eV	ΔG / eV	<O-C-O	C-O_b / Å	TM-C / Å	μ_d	q(CO_2)
Sc	−0.84	−0.16	139	1.28	2.42	0.08	−0.68
Ti	−1.58	−0.90	133	1.34	2.05	0.00	−0.82
V	−0.08	0.60	177	1.18	3.19	2.09	−0.06
Cr	−0.11	0.57	179	1.18	3.40	3.25	−0.02
Mn	−0.10	0.58	180	1.21	3.44	2.93	−0.30
Fe	−0.10	0.58	180	1.18	3.32	1.86	−0.01
Co	0.93	1.61	180	1.18	3.24	0.70	−0.03
Ni	−0.13	0.55	179	1.18	3.24	0.00	−0.03
Cu	0.04	0.72	180	1.17	3.31	0.54	−0.02
Mo	−1.41	−0.73	131	1.37	2.03	0.26	−0.83
Ru	−0.11	0.57	147	1.22	2.16	0.75	−0.41
Rh	−0.18	0.50	176	1.18	3.22	0.00	−0.05
Pd	−0.13	0.55	179	1.18	3.32	0.00	−0.03
Ag	−0.17	0.51	179	1.18	4.20	0.00	−0.01
W	−1.92	−1.24	129	1.43	2.02	0.30	−0.93
Os	−0.74	−0.06	139	1.30	2.02	0.00	−0.52
Ir	−0.19	0.49	176	1.18	3.28	0.00	−0.04
Pt	−0.14	0.54	178	1.18	3.35	0.00	−0.03
Au	−0.12	0.56	180	1.18	3.44	0.00	−0.01

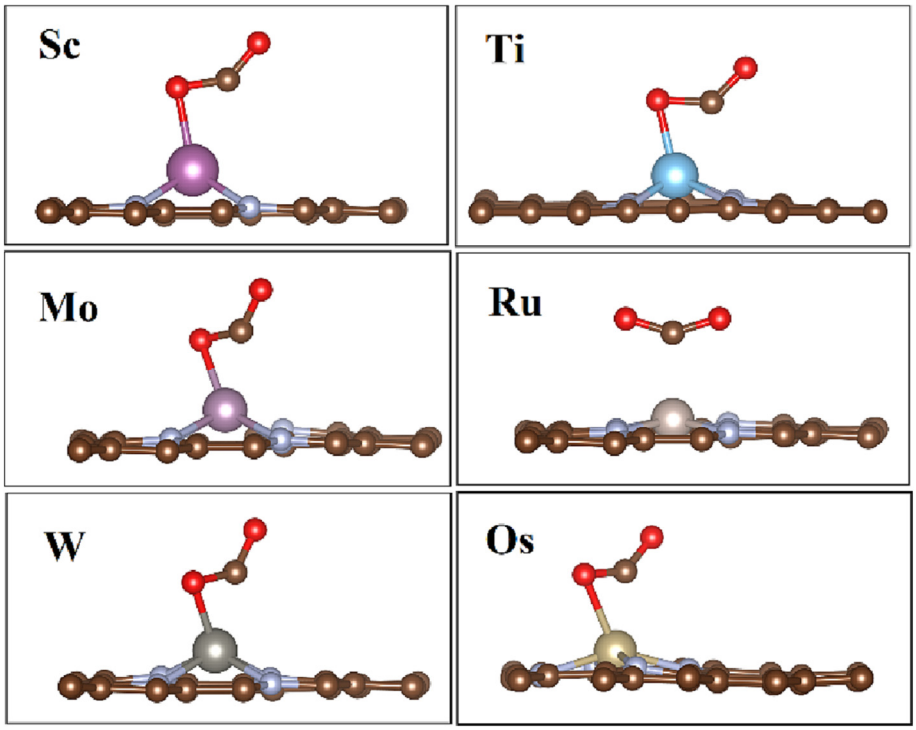

Fig. 1. Structure of CO_2 adsorbed on TM@4N-Gr for cases where the molecule is activated for the CO_2RR in absence of solvent. Blue, brown and red represents N, C and O atoms respectively. (For interpretation of the references to colour in this figure legend, the reader is referred to the web version of this article.)

molecule. In particular, Sc, Ti, Mo, W, and Os bind CO_2 in a side-on mode, while Ru forms a symmetric M−CO_2 complex. In all cases the O-C-O bond is considerably reduced, from 180° to 130-140°. However, only in three cases the CO_2/TM@4N-Gr complex is very favourable: Ti (ΔG = −0.90 eV), Mo (ΔG = −0.73 eV); W (ΔG = −1.24 eV). In the other cases the CO_2 molecule is activated, but ΔG is close to zero (Sc, Os) or even positive (Ru) indicating the formation of weakly stable or metastable complexes. These results confirm the difficulty to activate the CO_2 molecule and that very few systems have the required electronic characteristics to properly bind and distort this very stable molecule.

In the following we will concentrate our attention to these species, as it is unlikely that SACs that cannot bind and activate the CO_2 molecule can be active in CO_2RR.

3.1.2. Role of reaction intermediates

The next step of the CO_2RR is the first hydrogenation, and it is usually assumed that this results in the formation of COOH. Of course, the carboxylic path is not the only one, as the reaction can also proceed following the formate path (HCOO) [59], or via CO_2 dissociation which can be a main path in methane formation [60]. Normally the COOH path is preferred, but one should not forget the possible formation of another isomer, OCHO. Some recent studies have shown that the OCHO intermediate can be more stable than the COOH one [61]. Here we considered the competitive formation of COOH and OCHO for the six TM@4N-Gr SACs that activate CO_2 (Sc, Ti, Mo, Ru, W and Os), and for Ni@4N-Gr which is chosen as representative of inactive SACs (see Table 2 and Fig. 2 for adsorption and Gibbs free energies and the corresponding struc-

tures). The properties of some other, less stable, isomers of the COOH intermediate on the Mo- and W@4N-Gr complexes are given in Table S1 and Figure S1.

From Table 2 it appears that the formation of OCHO is preferred over that of COOH for Sc, Ti, Ni, Mo and W, while COOH formation is energetically preferred only for Ru and Os. Our results are consistent with previous theoretical studies on the same systems [18]. The fact that the OCHO intermediate is more stable than the COOH one implies, of course, a different reaction path than often assumed in many computational studies of the CO_2RR. Needless to say, this may lead to completely wrong conclusions about the potential activity of SACs in this particular reaction.

3.2. Role of water

3.2.1. Water as a ligand

As we mentioned in the Introduction, the CO_2RR on SACs occurs in water and water can have a twofold effect, that of solvating the various intermediates, but also to act as a ligand that interacts directly and competes with the CO_2 molecule to bind to the active site. TM atoms embedded in 4N-Gr are usually in a positive oxidation state [62] and water can interact electrostatically with these sites, forming stable aquo-complexes. To the best of our knowledge, the role of water as possible ligand in CO_2RR has not been considered so far.

Electrocatalytic reaction occur on a solid electrode. The surface of the electrode can be solvated and be in contact with liquid water. This is what is accounted for in classical solvation models. However, layered materials such as graphene can also be intercalated by small molecules diffusing between the layers. In this context, if a small amount of water can diffuse between two graphene layers it can also interact chemically with an embedded TM atom. What we want to address with our model is the possibility for the TM atoms to bind water molecules on both sides, where on one side the molecules are coming from the liquid phase, and in the other they are present as a consequence of an intercalation process.

Since the structures of TM@4N-Gr catalysts are planar or nearly planar (in some cases the TM atom is protruding from the graphene plane, see Figs. 1 and 2), in principle water can adsorb on both sides of the graphene plane: if the TM is perfectly aligned with the planar 4 N-Gr structure the situation is symmetric, but when the TM atom is displaced from the graphene plane this gives rise to two different isomers. In Table S2 and Figure S2 we report the results of the calculations where water has been adsorbed on the catalysts, either above or below the graphene layer. In some cases, the binding of water to the TM is quite strong, see for instance Sc@4N-Gr and Ti@4N-Gr, where $\Delta E_{ads}(H_2O)$ is about −1 eV. For Mo@4N-Gr and W@4N-Gr the adsorption energy of water is about −0.6/−0.7 eV. Notice that for some catalysts (*e.g.*, Sc) the binding of water is stronger than that of CO_2 (see also Table 1). When H_2O binds strongly it is coordinated to the TM atom *via* O, typical of aquo-complexes. In the other cases the binding is *via* H and the bonding is weaker, Table S2. Entropic effects considerably reduce the strength of the interaction, and the Gibbs free energy for water adsorption is negative only for Sc, Ti, and, to less extent, W, Table S2.

These results show that water can act as a labile ligand that, in some cases, can compete with CO_2. Also, water can bind together with CO_2. CO_2 has been adsorbed on the seven SACs considered by adding one water molecule on the opposite site of the graphene plane, see Figure S3 and Table S3. As a general result, the presence of a water molecule bound to the TM center lowers the strength of the bond of CO_2 to the catalyst, suggesting that CO_2 and H_2O can compete for adsorption on the catalyst surface; not surprisingly the effect is more pronounced for TM atoms that bind H_2O more strongly. This is a typical manifestation of the bond order conservation principle [63,64]. Of course, there is hardly any effect of water on CO_2 adsorption for Ni and Ru complexes, as both these TMs bind water very weakly.

Not surprisingly similar trends have been observed for the COOH and OCHO reaction intermediates, Table S4 and Figure S4 (here water has been adsorbed on opposite site of the active center). However, no effect has been found on the relative stability of the two isomers: the intermediate that is most stable on the dry catalyst remains the most stable one also in presence of one water molecule bound to the TM atom.

3.2.2. CO_2 activation in presence of water: Solvation versus coordination

In this Section we consider the effect of water. The treatment of solvent effects is complex, as it implies the simulation of solid/liquid interfaces, including dynamical effects *via ab-initio* molecular dynamics [65–67]. Since these are computationally rather intensive, alternative approaches have been suggested, including the implicit solvent model [68–72], or more accurate models where the water molecules are considered explicitly. For instance, one can approximate the solvation environment with a static array of water molecules; this is sometimes referred to as the water bilayer model [73–75]. However, also this approach is not free from limitations, such as the problem of strain at the interface. Another, simpler, approach has been proposed recently and assumes that main effect of the solvent is restricted to a small optimum number of water molecules. It has been suggested that three water molecules are enough to provide the most important solvation effects [76,77]. For this reason, the method has been named microsolvation model, and, according to some estimates, it provides results of comparable accuracy to those of the water bilayer model [77].

We adopted the microsolvation model to estimate the solvent effect on the stability of the intermediates considered in the CO_2RR (i.e. the CO_2/TM@4N-Gr complexes that bind and activate CO_2). In some cases, water acts only as a solvent and interacts weakly with the complex without forming a direct bond with the TM atom, Table 3 and Fig. 3. In the other cases, at least one water molecule binds sufficiently strongly with the TM center to act as a ligand, Table 4 and Fig. 4. We classify these systems as "solvation" or "coordination + solvation" complexes, since water can have a two-

Table 2
Relative stability and TM magnetization of COOH and OCHO intermediates for the CO_2RR in absence of solvent.

	COOH			OCHO		
TM	ΔE_{ads} / eV	ΔG / eV	μ_d	E_{ads} / eV	ΔG / eV	μ_d
Sc	−1.38	−0.35	0.00	−3.01	−2.00	0.00
Ti	−1.57	−0.54	0.43	−2.61	−1.61	0.54
Ni	1.04	2.07	0.51	0.78	1.79	0.25
Mo	−1.45	−0.41	0.00	−2.21	−1.20	0.39
Ru	−0.99	0.04	0.45	−0.16	0.85	0.82
W	−1.96	−0.92	0.00	−2.60	−1.59	0.68
Os	−1.12	−0.09	0.58	−0.71	0.30	0.63

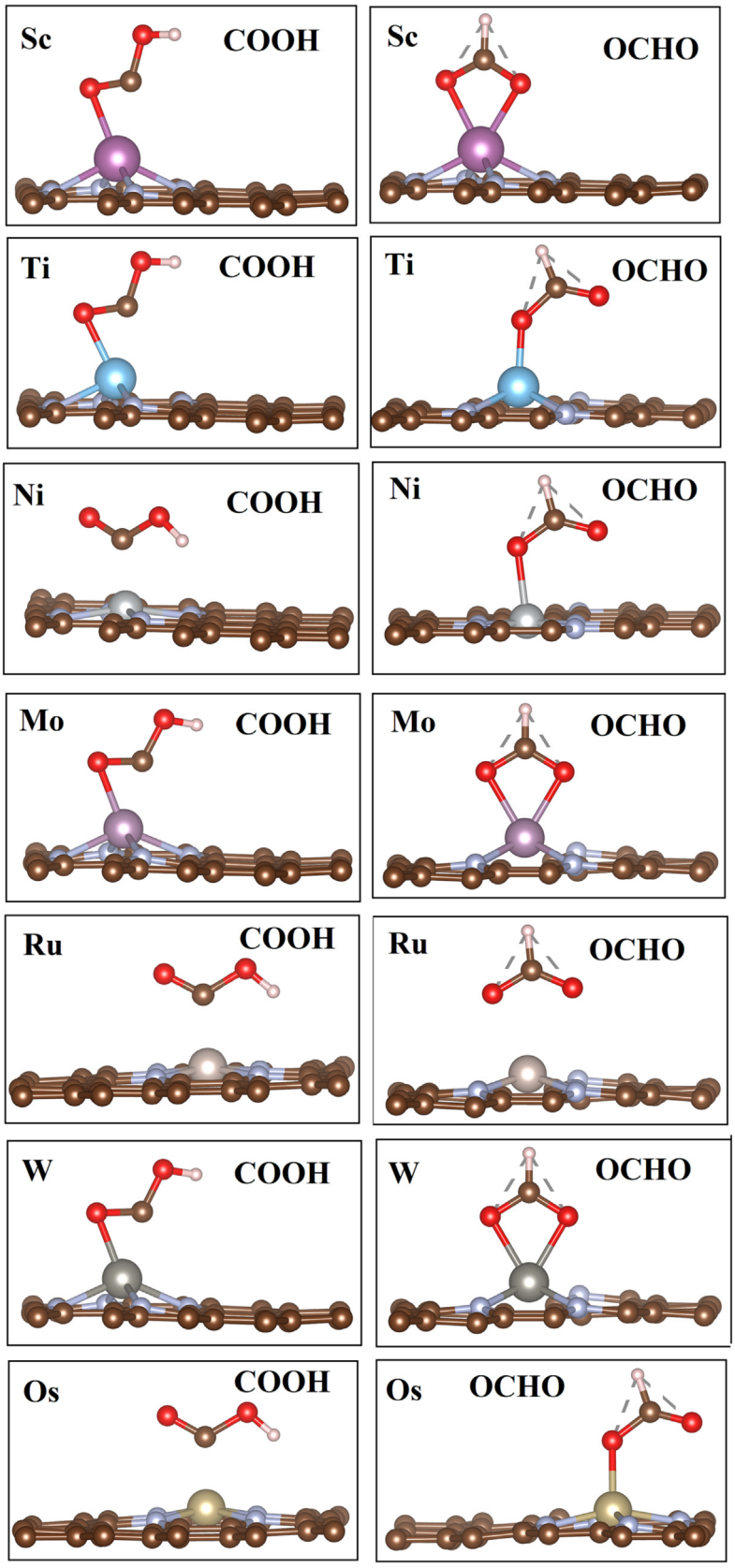

Fig. 2. COOH versus OCHO reaction intermediates on TM@4N-Gr for the CO_2RR in absence of solvent.

Table 3
Effect of water on CO_2 adsorption: adsorption energies, E^a_{ads} (CO_2), and adsorption free energies, ΔG (CO_2).

	Solvation		Coordination + Solvation	
TM	$E^a_{ads}(CO_2)$ / eV	ΔG^a (CO_2)/ eV	$E^a_{ads}(CO_2)$ / eV	ΔG^a (CO_2)/ eV
Sc	Unstable		−0.02	0.66
Ti	Unstable		−0.79	−0.11
Ni	0.06	0.74	unstable	
Mo	−1.11	−0.43	−1.44	−0.76
Ru	−0.19	0.49	−0.09	0.60
W	−1.36	−0.68	−1.77	−1.08
Os	−0.67	0.01	−0.11	0.57

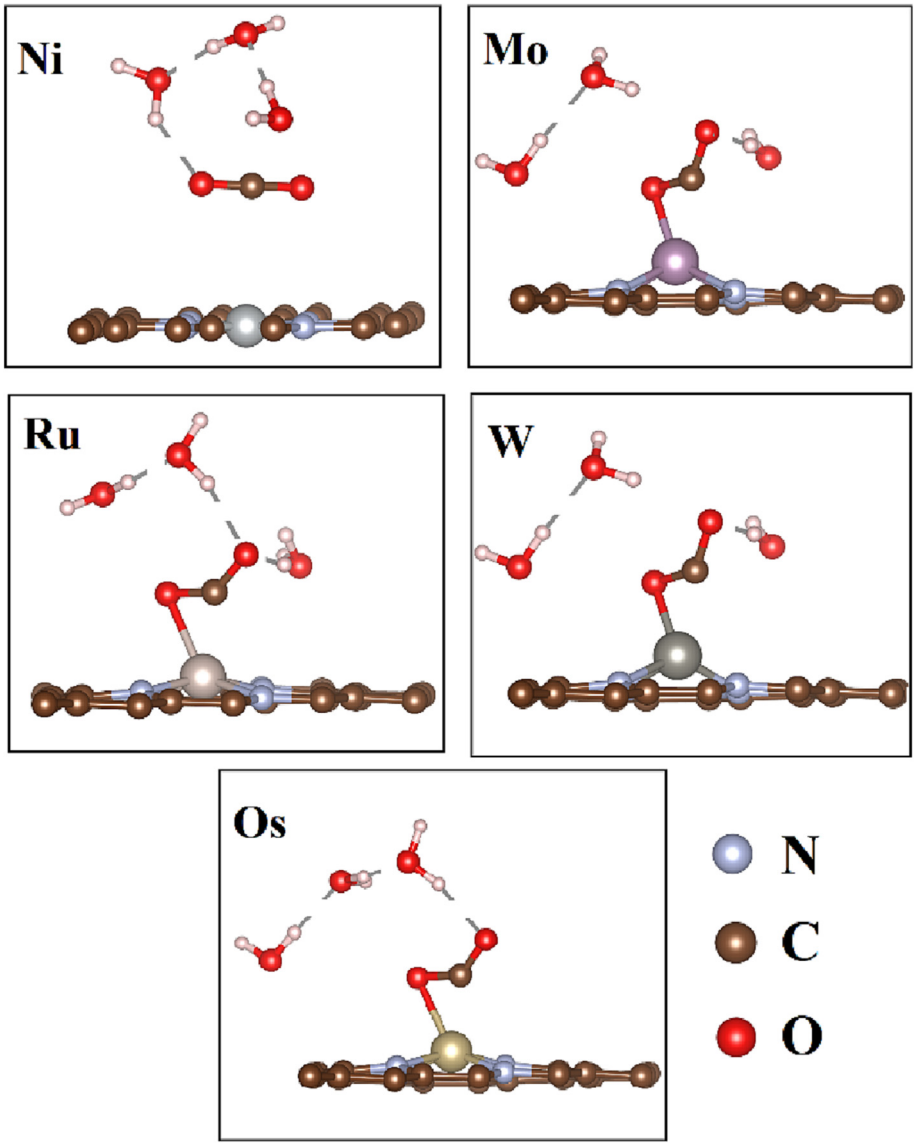

Fig. 3. Microsolvation models of CO_2 adsorption on TM@4N-Gr: "solvation" case.

fold effect. It must be underlined that our aim is not to exhaustively describe the solvation of simulated species, but rather to adopt a simple scheme able to discriminate when water acts a solvent only and when it coordinates to the metal. Indeed, solvation shells are often complex, and more than just a few water molecules are usually involved. In addition, static approaches neglect dynamical effects which are important when interfacing with water [78–80].

In Table 3, we report the energy of adsorption of CO_2, $E^a_{ads}(CO_2)$, when water acts only as a solvent, see "solvation", while when water also coordinates to the metal, we refer to "coordination + solvation". The adsorption energies and structures of water on the bare catalysts (without CO_2 adsorbed), used as a reference, are reported in Table S5 and Figure S5 respectively.

From Table 3 it is clear that "solvation" reduces the adsorption energies for all cases and hence results in a weaker interaction of

Table 4
Effect of water ("solvation") on COOH or OCHO adsorption: adsorption energies, E^{a}_{ads}, and adsorption free energies, ΔG. The TM atom magnetization is also given.

Solvation						
TM	COOH			OCHO		
	ΔE_{ads} / eV	ΔG / eV	μ_d	ΔE_{ads} / eV	ΔG / eV	μ_d
Sc	−0.19	0.84	0.00	Unstable		
Ti	−0.89	0.17	0.36	−1.31	−0.30	0.47
Ni	0.50	1.53	0.00	0.37	1.38	0.00
Mo	−1.57	−0.54	0.00	−1.02	−0.02	0.00
Ru	−0.55	0.48	0.00	−0.18	0.82	0.00
W	−1.78	−0.75	0.00	−1.47	−0.46	0.66
Os	−0.63	0.41	0.58	−0.20	0.81	0.67

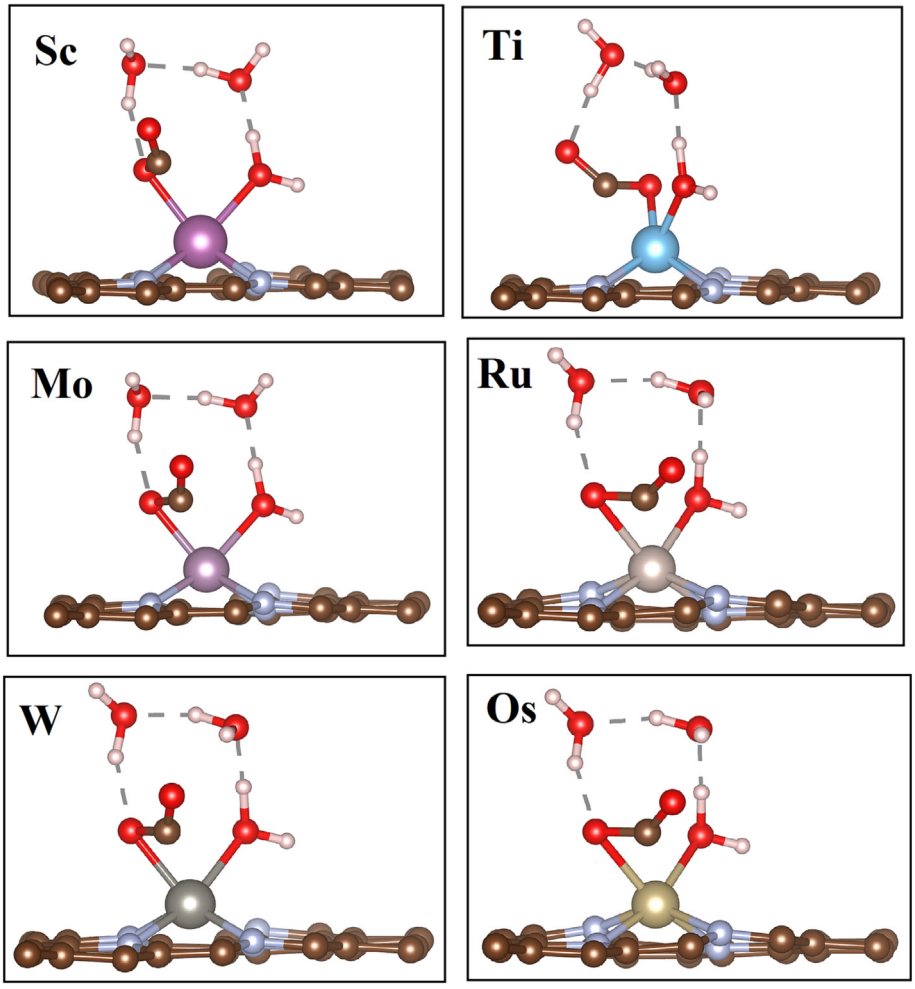

Fig. 4. Microsolvation models of CO_2 adsorption on TM@4N-Gr: "coordination + solvation" case.

CO_2 with the catalysts. For instance, on Mo@4N-Gr the adsorption energy of CO_2 goes from −1.41 eV on the dry catalyst, Table 1, to −1.11 eV with the solvent, Table 3; on W@4N-Gr we go from −1.92 eV to −1.36 eV. The effect is present but smaller on Ni, Ru, and Os catalysts, see Table 1 and Table 3. Pure solvation is not observed for Sc and Ti, since the resulting complexes are unstable. For these two systems (and for all other TMs except Ni) one water molecule binds directly to the TM center, Fig. 4, and thus acts simultaneously as solvent and as ligand (see also Table 4, "coordination + solvation").

The "coordination + solvation" situation is preferred for Sc, Ti, Mo and W; all these TMs binds water strongly. On the contrary, pure "solvation" (Table 3, Fig. 3) is preferable for Ni, Ru and Os, TMs that bind water weakly. As for the "solvation" case, also for "coordination + solvation" complexes the presence of water results in a weaker bonding of CO_2 to the active site. For Sc@4N-Gr, $E_{ads}(CO_2)$ goes from −0.84 eV for the dry catalyst, Table 1, to −0.02 eV when water is considered, Table 4; a similar situation is found for Ti@4N-Gr where $E_{ads}(CO_2)$ goes from −1.58 eV, Table 1, to −0.79 eV, Table 4. On the contrary, much less pronounced is the effect of water on the SACs based on Mo, Ru, W and Os, see Table 1 and Table 3. This suggests that the use of scaling relations may be problematic since the effect of water as a ligand is not the same for all complexes.

To summarize, both "solvation" and "coordination + solvation" cases result in less negative CO_2 adsorption energies (and conse-

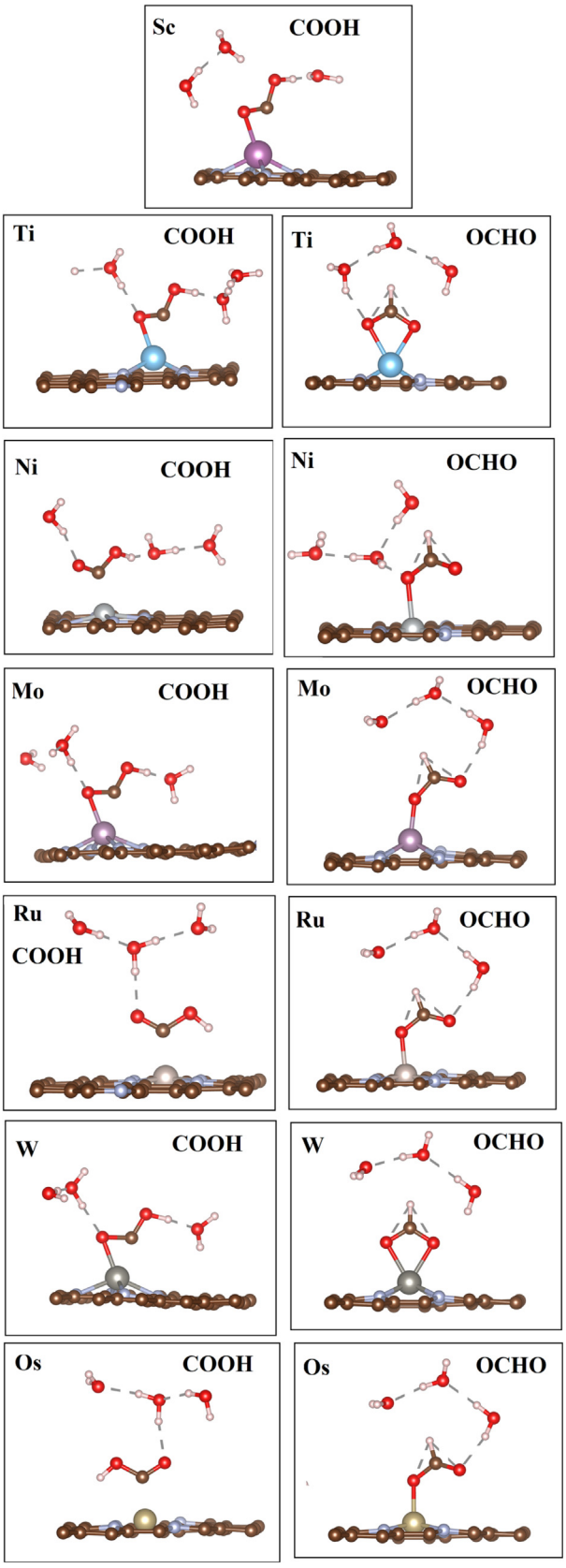

Fig. 5. Microsolvation models of COOH and OCHO reaction intermediates on TM@4N-Gr: "solvation" case.

quently less favourable adsorption free energies), making CO_2 adsorption weaker compared to the dry catalysts.

3.2.3. Reaction intermediates in presence of water: Solvation versus coordination

The role of water has also been studied for the two reaction intermediates considered in this study, COOH and OCHO. Following the same lines discussed in the previous Section, water can act as a solvent only, or as a solvent and a ligand at the same time. Table 4 reports the adsorption energies, adsorption free energies and TM magnetization for both COOH and OCHO intermediates showing cases where water acts exclusively as a solvent ("solvation"); the corresponding structures are shown in Fig. 5. Table 5 and Fig. 6 contain the same info but for the structures where "coordination + solvation" is observed.

Similarly to CO_2 adsorption, also for step 2 of the CO_2RR, formation of COOH or OCHO intermediates, the "coordination + solvation" case is preferred for TMs that bind water strongly, while pure "solvation" is preferred for TMs that adsorbs water weakly, Tables 4-5. In general, the presence of water does not alter the relative stability of the reaction intermediates found for the dry catalyst (but there are exceptions). However, the effect is not same for all catalysts. On Ti@4N-Gr, for instance, the difference in stability for the two intermediates on the dry catalyst, 1.04 eV (ΔE_{ads}(OCHO) = −2.61 eV; ΔE_{ads}(COOH) = −1.57 eV, Table 2) increases to 1.48 eV with the solvent (ΔE_{ads}(OCHO) = −2.02 eV; ΔE_{ads}(COOH) = −0.54 eV, Table 5); on Mo@4N-Gr the effect is similar: on the dry catalyst OCHO is 0.76 eV more stable than COOH (ΔE_{ads}(OCHO) = −2.21 eV; ΔE_{ads}(COOH) = −1.45 eV, Table 2), while with the solvent the difference is 0.94 eV (ΔE_{ads}(OCHO) = −2.31 eV; ΔE_{ads}(COOH) = −1.37 eV, Table 5). However, there are also cases where the order of stability of the two intermediates is reversed after the addition of water: on the Os@4N-Gr dry catalyst COOH is more stable than OCHO by 0.41 eV (ΔE_{ads}(COOH) = −1.12 eV; ΔE_{ads}(OCHO) = −0.71 eV, Table 2), while in the presence of water the OCHO intermediate is 0.09 eV more stable (ΔE_{ads}(OCHO) = −0.89 eV; ΔE_{ads}(COOH) = −0.80 eV, Table 5). This shows, once more, that each SAC has a different behaviour, due to the specific interaction of the *n*d shell of the TM atom with the ligands.

4. Conclusions

In this work we have investigated the initial steps of the CO_2 electro-catalytic reduction on TM atoms embedded in nitrogen-doped graphene (TM@4N-Gr), by means of density functional theory simulations. We analysed some relevant aspects of the reactivity of single atom catalysts that are often neglected in the current studies on the problem. In particular, we have addressed three crucial points.

(1) The role of water. We found cases where water acts not only as a solvent that binds *via* hydrogen bonds and dispersion forces, but also as a ligand when the TM-H_2O interaction is strong. In this case water can compete with CO_2 or with the reaction intermediates in binding the TM center. In general, the presence of water in the simulation results in less negative free energies of adsorption of CO_2, COOH, or OCHO species, showing an overall destabilizing effect with non-negligible consequences on the thermodynamic barriers of the CO_2 reduction. Also, the relative order of stability of the competing COOH and OCHO intermediates can change going from the dry SAC model (no solvent) to the solvated model. While for most of the cases examined the order of stability is the same, there are also cases, such as Os@4N-Gr, where the presence of water has the effect to change the order of stability and to modify the predicted mechanism of the reaction.

(2) The first step of the reaction consists in binding and activating the CO_2 molecule. We found that, out of 19 TM@4N-Gr complexes considered, only in a minority of cases CO_2 is significantly bound and activated (in this case the structure deviates

Table 5
Effect of water ("coordination + solvation") on COOH or OCHO adsorption: adsorption energies, E^{a}_{ads}, and adsorption free energies, ΔG. The TM atom magnetization is also given.

TM	Coordination + Solvation					
	COOH			OCHO		
	ΔE_{ads} / eV	ΔG / eV	μ_d	ΔE_{ads} / eV	ΔG / eV	μ_d
Sc	−0.35	0.69	0.00	−2.05	−1.04	0.00
Ti	−0.54	0.50	0.00	−2.02	−1.02	0.42
Ni	unstable			1.63	2.64	1.53
Mo	−1.37	−0.33	0.00	−2.31	−1.31	0.00
Ru	−0.59	0.45	0.00	−0.24	0.77	0.00
W	−1.62	−0.58	0.00	−2.43	−1.42	0.00
Os	−0.80	0.23	0.00	−0.89	0.12	0.00

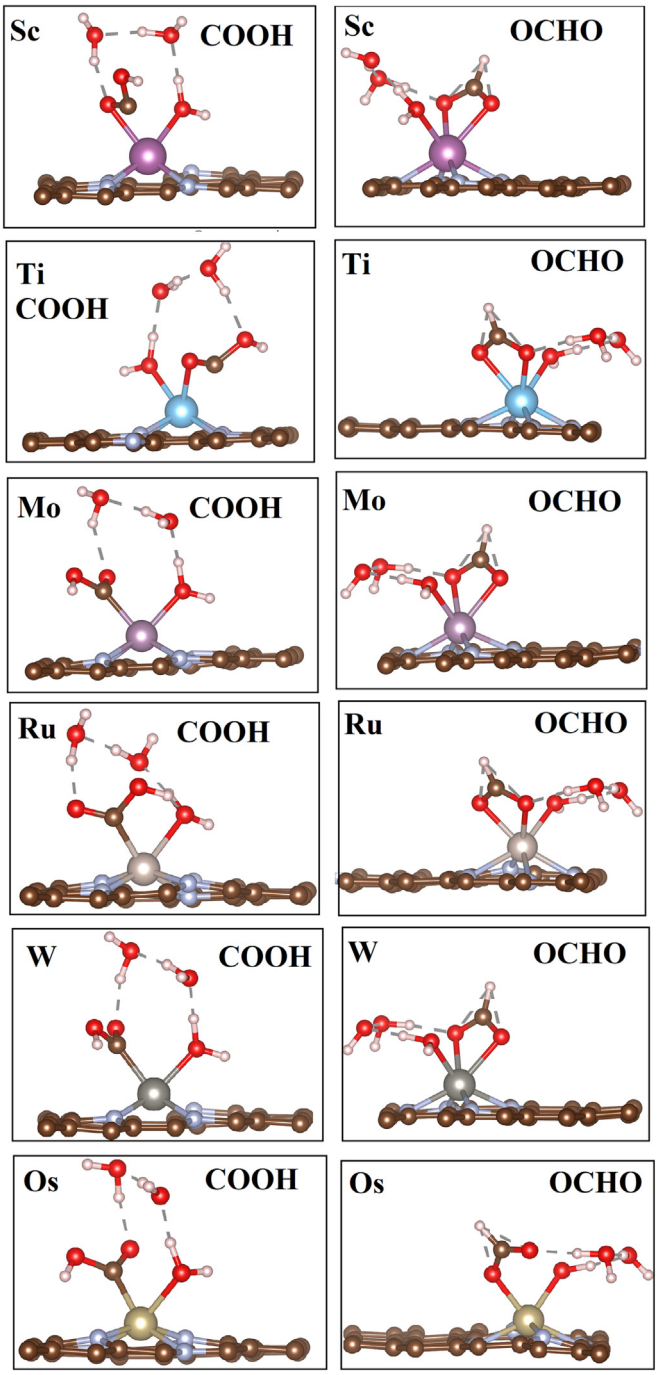

Fig. 6. Microsolvation models of COOH and OCHO reaction intermediates on TM@4N-Gr: "coordination + solvation" case.

from that of the linear gas-phase molecule). In water, in order to bind to the TM active site, the CO_2 molecule needs to displace the water molecules directly bound to the metal center. This is not easy since in many cases water binds to SACs more strongly than CO_2.

(3) The last aspect investigated is the possible formation of more than one intermediate in a given reaction step, giving rise to different reaction paths. We have considered the competing formation of COOH and OCHO intermediates (first reaction step) for a selected number of TM@4N-Gr complexes, finding that the OCHO complex is more stable in most cases, at variance with the usual assumption that the reaction proceeds *via* formation of COOH. Similar results have been reported in the literature [18,61]. However, as we mentioned before, water has an effect on the relative stability of the COOH and OCHO intermediates which varies from case to case. This is a problem for the identification of scaling relationships, since the behaviour can be markedly dependent on the TM atom. What remains to be evaluated is the effect of water on the kinetic barriers for the reaction, an aspect that will be considered in future studies.

In conclusion, SACs have a rich chemistry and their modelling with first principles calculations requires to include all variables in order to reach meaningful conclusions [81]. Screening of large numbers of potential candidates as catalysts for the reaction that do not accounts for this complexity can lead to questionable predictions. Furthermore, the work confirms the similarity of the chemistry of SACs embedded in graphene-based substrates with that of coordination compounds.

Data availability

Data will be made available on request.

Declaration of Competing Interest

The authors declare that they have no known competing financial interests or personal relationships that could have appeared to influence the work reported in this paper.

Acknowledgement

DM thanks the Science and Engineering Research Board (SERB), Govt. of India, for the SIRE fellowship (award no. SIR/2022/000690) which supported her visit to University Milano-Bicocca for three months where the entire work has been carried out. We acknowledge the financial support from CARIPLO Foundation, project "Carbon dioxide conversion into energy-rich molecules with tailored catalysts". Access to the CINECA supercomputing resources was granted *via* ISCRAB. We also thank the COST Action 18234 supported by COST (European Cooperation in Science and Technology).

Appendix A. Supplementary data

Supplementary data to this article can be found online at https://doi.org/10.1016/j.jcat.2023.04.002.

References

[1] A. Rendón-Calle, S. Builes, F. Calle-Vallejo, A brief review of the computational modeling of CO_2 electroreduction on Cu electrodes, Curr. Opin. Electrochem. 9 (2018) 158–165, https://doi.org/10.1016/j.coelec.2018.03.012.

[2] D.T. Whipple, P.J.A. Kenis, Prospects of CO_2 Utilization via Direct Heterogeneous Electrochemical Reduction, J. Phys. Chem. Lett. 1 (2010) 3451–3458, https://doi.org/10.1021/jz1012627.

[3] K.P. Kuhl, E.R. Cave, D.N. Abram, T.F. Jaramillo, New insights into the electrochemical reduction of carbon dioxide on metallic copper surfaces, Energy Environ. Sci. 5 (2012) 7050–7059, https://doi.org/10.1039/C2EE21234J.

[4] K.P. Kuhl, T. Hatsukade, E.R. Cave, D.N. Abram, J. Kibsgaard, T.F. Jaramillo, Electrocatalytic conversion of carbon dioxide to methane and methanol on transition metal surfaces, J. Am. Chem. Soc. 136 (2014) 14107–14113, https://doi.org/10.1021/ja505791r.

[5] S.A. Akhade, W. Luo, X. Nie, A. Asthagiri, M.J. Janik, Theoretical insight on reactivity trends in CO_2 electroreduction across transition metals, Catal. Sci. Technol. 6 (2016) 1042–1053, https://doi.org/10.1039/C5CY01339A.

[6] C.S. Chen, A.D. Handoko, J.H. Wan, L. Ma, D. Ren, B.S. Yeo, Stable and selective electrochemical reduction of carbon dioxide to ethylene on copper mesocrystals, Catal. Sci. Technol. 5 (2015) 161–168, https://doi.org/10.1039/C4CY00906A.

[7] Y. Hori, I. Takahashi, O. Koga, N. Hoshi, Electrochemical reduction of carbon dioxide at various series of copper single crystal electrodes, J. Mol. Catal. A: Chem. 199 (2003) 39–47, https://doi.org/10.1016/S1381-1169(03)00016-5.

[8] S.T. Ahn, I. Abu-Baker, G.T.R. Palmore, Electroreduction of CO_2 on polycrystalline copper: effect of temperature on product selectivity, Catal. Today 288 (2017) 24–29, https://doi.org/10.1016/j.cattod.2016.09.028.

[9] G. Zhu, Y. Li, H. Zhu, H. Su, S.H. Chan, Q. Sun, Curvature-dependent selectivity of CO_2 electrocatalytic reduction on cobalt porphyrin nanotubes, ACS Catal. 6 (2016) 6294–6301, https://doi.org/10.1021/acscatal.6b02020.

[10] C. Liu, B.C. Colón, M. Ziesack, P.A. Silver, D.G. Nocera, Water splitting-biosynthetic system with CO_2 reduction efficiencies exceeding photo synthesis, Science 352 (2016) 1210–1213, https://doi.org/10.1126/science.aaf5039.

[11] F. Pan, B. Li, W. Deng, Z. Du, Y. Gang, G. Wang, Y. Li, Promoting electrocatalytic CO_2 reduction on nitrogen-doped carbon with sulfur addition, Appl. Catal. B: Environ. 252 (2019) 240–249, https://doi.org/10.1016/j.apcatb.2019.04.025.

[12] T. Ma, Q. Fan, X. Li, J. Qiu, T. Wu, Z. Sun, Graphene-based materials for electrochemical CO_2 reduction, J. CO_2 Util. 30 (2019) 168–182, https://doi.org/10.1016/j.jcou.2019.02.001.

[13] X. Yang, A. Wang, B. Qiao, J. Li, J. Liu, T. Zhang, Single-Atom Catalysts: A New Frontier in Heterogeneous Catalysis, Acc. Chem. Res. 46 (2013) 1740–1748, https://doi.org/10.1021/ar300361m.

[14] B. Qiao, A. Wang, X. Yang, L.F. Allard, Z. Jiang, Y. Cui, J. Liu, J. Li, T. Zhang, Single-atom catalysis of CO oxidation using Pt_1/FeO_x, Nat. Chem. 3 (2011) 634–641, https://doi.org/10.1038/nchem.1095.

[15] S. Mitchell, J. Pérez-Ramírez, Atomically precise control in the design of low-nuclearity supported metal catalysts, Nat. Rev. Mater. 6 (2021) 969–985, https://doi.org/10.1038/s41578-021-00360-6.

[16] M. Umeda, Y. Niitsuma, T. Horikawa, S. Matsuda, M. Osawa, Electrochemical Reduction of CO_2 to Methane on Platinum Catalysts without Overpotentials: Strategies for Improving Conversion Efficiency, ACS Appl. Energy Mater. 3 (2020) 1119–1127, https://doi.org/10.1021/acsaem.9b02178.

[17] E.R. Cave, J.H. Montoya, K.P. Kuhl, D.N. Abram, T. Hatsukade, C. Shi, C. Hahn, J.K. Nørskov, T.F. Jaramillo, Electrochemical CO_2 Reduction on Au Surfaces: Mechanistic Aspects Regarding the Formation of Major and Minor Products, Phys. Chem. Chem. Phys. 19 (2017) 15856–15863, https://doi.org/10.1039/C7CP02855E.

[18] Y. Yang, J. Li, C. Zhang, Z. Yang, P. Sun, S. Liu, Q. Cao, Theoretical Insights into Nitrogen-Doped Graphene-Supported Fe Co, and Ni as Single-Atom Catalysts for CO2 Reduction Reaction, J. Phys. Chem. C 126 (2022) 4338–4346, https://doi.org/10.1021/acs.jpcc.1c09740.

[19] P. Su, K. Iwase, S. Nakanishi, K. Hashimoto, K. Kamiya, Nickel-Nitrogen-Modified Graphene: An Efficient Electrocatalyst for the Reduction of Carbon Dioxide to Carbon Monoxide, Small 12 (2016) 6083–6089, https://doi.org/10.1002/smll.201602158.

[20] M. Liu, Y. Pang, B. Zhang, P.D. Luna, O. Voznyy, J. Xu, X. Zheng, C.T. Dinh, F. Fan, C. Cao, F.P.G.D. Arquer, T.S. Safaei, A. Mepham, A. Klinkova, E. Kumacheva, T. Filleter, D. Sinton, S.O. Kelley, E.H. Sargent, Enhanced Electrocatalytic CO_2 Reduction via Field-Induced Reagent Concentration, Nature 537 (2016) 382–386, https://doi.org/10.1038/nature19060.

[21] Y.Y. Birdja, E. Pérez-Gallent, M.C. Figueiredo, A.J. Göttle, F. Calle-Vallejo, M.T.M. Koper, Advances and Challenges in Understanding the Electrocatalytic Conversion of Carbon Dioxide to Fuels, Nat. Energy 4 (2019) 732–745, https://doi.org/10.1038/s41560-019-0450-y.

[22] N. Cheng, S. Stambula, D. Wang, M.N. Banis, J. Liu, A. Riese, B. Xiao, R. Li, T.K. Sham, L.M. Liu, G.A. Botton, X. Sun, Platinum single-atom and cluster catalysis of the hydrogen evolution reaction, Nat. Commun. 7 (2016) 13638, https://doi.org/10.1038/ncomms13638.

[23] S. Sun, G. Zhang, N. Gauquelin, N. Chen, J. Zhou, S. Yang, W. Chen, X. Meng, D. Geng, M.N. Banis, R. Li, S. Ye, S. Knights, G.A. Botton, T. Sham, X. Sun, Single-atom Catalysis Using Pt/Graphene Achieved through Atomic Layer Deposition, Sci. Rep. 3 (2013) 1775, https://doi.org/10.1038/srep01775.

[24] J. Jones, H. Xiong, A.T. DeLaRiva, E.J. Peterson, H. Pham, S.R. Challa, G. Qi, S. Oh, M.H. Wiebenga, X.I. Pereira Hernández, Y. Wang, A.K. Datye, Thermally stable single-atom platinum-on ceria catalysts via atom trapping, Science 353 (2016) 150–154, https://doi.org/10.1126/science.aaf8800.

[25] M. Zhu, C. Cao, J. Chen, Y. Sun, R. Ye, J. Xu, Y. Han, Electronic Tuning of Cobalt Porphyrins Immobilized on Nitrogen-Doped Graphene for CO_2 Reduction, ACS Appl. Energy Mater. 2 (2019) 2435–2440, https://doi.org/10.1021/acsaem.9b00368.

[26] A. Liu, W. Guan, K. Wu, X. Ren, L. Gao, T. Ma, Density functional theory study of nitrogen-doped graphene as a high-performance electrocatalyst for CO_2RR, Appl. Surf. Sci. 540 (2021) 1483, https://doi.org/10.1016/j.apsusc.2020.148319.

[27] S. Liu, L. Cheng, K. Li, C. Yin, H. Tang, Y. Wang, Z. Wu, RuN_4 Doped Graphene Oxide, a Highly Efficient Bifunctional Catalyst for Oxygen Reduction and CO_2 Reduction from Computational Study, ACS Sustainable Chem. Eng. 7 (2019) 8136–8144, https://doi.org/10.1021/acssuschemeng.8b05729.

[28] G. Di Liberto, L.A. Cipriano, G. Pacchioni, Universal Principles for the Rational Design of Single Atom Electrocatalysts?, Handle with Care, ACS Catal 12 (2022) 5846–5856, https://doi.org/10.1021/acscatal.2c01011.

[29] Z. Du, X. Chen, W. Hu, C. Chuang, S. Xie, A. Hu, W. Yan, X. Kong, X. Wu, H. Ji, L.J. Wan, Cobalt in Nitrogen-Doped Graphene as Single-Atom Catalyst for High-Sulfur Content Lithium-Sulfur Batteries, J. Am. Chem. Soc. 141 (2019) 3977–3985, https://doi.org/10.1021/jacs.8b12973.

[30] S. Zhou, L. Shang, Y. Zhao, R. Shi, G.I.N. Waterhouse, Y. Huang, L. Zheng, T. Zhang, Pd Single-Atom Catalysts on Nitrogen-Doped Graphene for the Highly Selective Photothermal Hydrogenation of Acetylene to Ethylene, Adv. Mater. 31 (2019) 1900509, https://doi.org/10.1002/adma.201900509.

[31] V. Fung, G. Hu, Z. Wu, D. Jiang, Descriptors for Hydrogen Evolution on Single Atom Catalysts in Nitrogen-Doped Graphene, J. Phys. Chem. C 124 (2020) 19571–19578, https://doi.org/10.1021/acs.jpcc.0c04432.

[32] L. Liu, S. Liu, L. Li, H. Qi, H. Yang, Y. Huang, Z. Wei, L. Li, J. Xu, B. Liu, A general method to construct single-atom catalysts supported on N-doped graphene for energy applications, J. Mater. Chem. A 8 (2020) 6190–6195, https://doi.org/10.1039/C9TA11715F.

[33] R. Jayan, M.M. Islam, Single-Atom Catalysts for Improved Cathode Performance in Na–S Batteries: A Density Functional Theory (DFT) Study, J. Phys. Chem. C 125 (2021) 4458–4467, https://doi.org/10.1021/acs.jpcc.1c00467.

[34] W. Gong, F. Zhao, L. Kang, Novel nitrogen-doped Au-embedded graphene single-atom catalysts for acetylene hydrochlorination: A density functional theory study, Comput, Theor. Chem. 1130 (2018) 83–89, https://doi.org/10.1016/j.comptc.2018.03.015.

[35] D. Dao, L.A. Cipriano, G. Di Liberto, T.T.D. Nguyen, S. Ki, H. Son, G. Kim, K.H. Lee, J. Yang, Y. Yu, G. Pacchioni, I. Lee, Plasmonic Au nanoclusters dispersed in nitrogen-doped graphene as a robust photocatalyst for light-to-hydrogen conversion, J. Mater. Chem. A 9 (2021) 22810–22819, https://doi.org/10.1039/D1TA05445G.

[36] H. Wang, Y. Chen, X. Hou, C. Ma, T. Tan, Nitrogen-doped graphenes as efficient electrocatalysts for the selective reduction of carbon dioxide to formate in aqueous solution, Green Chem. 18 (2016) 3250–3256, https://doi.org/10.1039/C6GC00410E.

[37] C. Coperet, M. Chabanas, R.P. Saint-Arroman, J. Basset, Homogeneous and Heterogeneous Catalysis: Bridgingthe Gap through Surface Organometallic Chemistry, J. Angew. Chem. Int. Ed. 42 (2003) 156–181, https://doi.org/10.1002/anie.200390072.

[38] G.S. Parkinson, Single-Atom Catalysis: How Structure Influences Catalytic Performance, Catal. Lett. 149 (2019) 1137–1146, https://doi.org/10.1007/s10562-019-02709-7.

[39] G. Di Liberto, L.A. Cipriano, G. Pacchioni, Role of Dihydride and Dihydrogen Complexes in Hydrogen Evolution Reaction on Single-Atom Catalysts, J. Am. Chem. Soc. 143 (2021) 20431–20441, https://doi.org/10.1021/jacs.1c10470.

[40] L.A. Cipriano, G. Di Liberto, G. Pacchioni, Superoxo and Peroxo Complexes on Single-Atom Catalysts: Impact on the Oxygen Evolution Reaction, ACS Catal. 12 (2022) 11682–11691, https://doi.org/10.1021/acscatal.2c03020.

[41] P. Brimley, H. Almajed, Y. Alsunni, A.W. Alherz, Z.J.L. Bare, W.A. Smith, C.B. Musgrave, Electrochemical CO_2 Reduction over Metal-/Nitrogen-Doped Graphene Single-Atom Catalysts Modeled Using the Grand-Canonical Density Functional Theory, ACS Catal. 12 (2022) 10161–10171, https://doi.org/10.1021/acscatal.2c01832.

[42] W. Bi, X. Li, R. You, M. Chen, R. Yuan, W. Huang, X. Wu, W. Chu, C. Wu, Y. Xie, Surface Immobilization of Transition Metal Ions on Nitrogen-Doped Graphene Realizing High-Efficient and Selective CO_2 Reduction, Adv. Mater. 30 (2018) 1706617, https://doi.org/10.1002/adma.201706617.

[43] C. Zhang, S. Yang, J. Wu, M. Liu, S. Yazdi, M. Ren, J. Sha, J. Zhong, K. Nie, A.S. Jalilov, Z. Li, H. Li, B.I. Yakobson, Q. Wu, E. Ringe, H. Xu, P.M. Ajayan, J.M. Tour, Electrochemical CO_2 Reduction with Atomic Iron-Dispersed on Nitrogen-Doped Graphene, Adv. Energy Mater. 8 (2018) 1703487, https://doi.org/10.1002/aenm.201703487.

[44] R. Ma, K. Wang, C. Li, C. Wang, A. Habibi-Yangjeh, G. Shan, N-doped graphene for electrocatalytic $_O$2 and C_O2 reduction, Nanoscale Adv. 4 (2022) 4197–4209, https://doi.org/10.1039/D2NA00348A.
[45] G. Kresse, J. Furthmüller, Efficient iterative schemes for abinitio total-energy calculations using a plane-wave basis set, Phys. Rev. B 54 (1996) 11169–11186, https://doi.org/10.1103/PhysRevB.54.11169.
[46] G. Kresse, J. Furthmüller, Efficiency of ab-initio total energy calculations for metals and semiconductors using a plane-wave basis set, Comput. Mater. Sci. 6 (19961) 15−50, https://doi.org/10.1016/0927-0256(96)00008-0.
[47] P.E. Blöchl, Projector augmented-wave method, Phys. Rev. B 50 (1994) 17953–17979, https://doi.org/10.1103/PhysRevB.50.17953.
[48] J.P. Perdew, K. Burke, M. Ernzerhof, Generalized gradient approximation made simple, Phys. Rev. Lett. 77 (1996) 3865–3868, https://doi.org/10.1103/PhysRevLett.77.3865.
[49] S. Grimme, J. Antony, S. Ehrlich, H. Krieg, A consistent and accurate ab initio parametrization of density functional dispersion correction (DFT-D) for the 94 elements H-Pu, J. Chem. Phys. 132 (2010), https://doi.org/10.1063/1.3382344.
[50] G. Di Liberto, L.A. Cipriano, G. Pacchioni, Single atom catalysts: what matters most, the active site or the surrounding?, ChemCatChem 14 (2022) e2022006
[51] I. Barlocco, L.A. Cipriano, G. Di Liberto, G. Pacchioni, Modeling Hydrogen and Oxygen Evolution Reactions on Single Atom Catalysts with Density Functional Theory: Role of the Functional, Adv. Theory Simul. 2200513 (2022), https://doi.org/10.1002/adts.202200513.
[52] I. Barlocco, L.A. Cipriano, G. Di Liberto, G. Pacchioni, Does the Oxygen Evolution Reaction follow the classical OH*, O*, OOH* path on single atom catalysts?, J Catal. 417 (2023) 351–359, https://doi.org/10.1016/j.jcat.2022.12.014.
[53] J.K. Nørskov, T. Bligaard, A. Logadottir, J.R. Kitchin, J.G. Chen, S. Pandelov, U. Stimming, Trends in the Exchange Current for Hydrogen Evolution, J. Electrochem. Soc. 152 (2005) J23, https://doi.org/10.1149/1.1856988.
[54] http://webbook.nist.gov/chemistry/.
[55] J.K. Nørskov, J. Rossmeisl, A. Logadottir, L. Lindqvist, J.R. Kitchin, T. Bligaard, H. Jónsson, Origin of the Overpotential for Oxygen Reduction at a Fuel-Cell Cathode, J. Phys. Chem. B 108 (2004) 17886–17892, https://doi.org/10.1021/jp047349j.
[56] G. Liberto, R. Conte, M. Ceotto, "Divide-and-conquer" semiclassical molecular dynamics: An application to water clusters, J. Chem. Phys. 148 (2018), https://doi.org/10.1063/1.5023155.
[57] J. Greeley, J.K. Nørskov, Electrochemical dissolution of surface alloys in acids: Thermodynamic trends from first-principles calculations, Electrochim. Acta 52 (2007) 5829–5836, https://doi.org/10.1016/j.electacta.2007.02.082.
[58] M. López, K.S. Exner, F. Viñes, F. Illas, Computational Pourbaix Diagrams for MXenes: A Key Ingredient toward Proper Theoretical Electrocatalytic Studies, Adv. Theory Simul. 2200217 (2022), https://doi.org/10.1002/adts.202200217.
[59] A. Jurado, Á. Morales-García, F. Viñes, F. Illas, Molecular Mechanism and Microkinetic Analysis of the Reverse Water Gas Shift Reaction Heterogeneously Catalyzed by the Mo_2C Mxene, ACS Catal. 12 (24) (2022) 15658–15667, https://doi.org/10.1021/acscatal.2c04489.
[60] P. Lozano-Reis, H. Prats, P. Gamallo, F. Illas, R. Sayós, Multiscale Study of the Mechanism of Catalytic CO_2 Hydrogenation: Role of the Ni(111) Facets, ACS Catal. 10 (15) (2020) 8077–8089, https://doi.org/10.1021/acscatal.0c01599.
[61] P. Huang, M. Cheng, H. Zhang, M. Zuo, C. Xiao, Y. Xie, Single Mo atom realized enhanced CO_2 electro-reduction into formate on N-doped graphene, Nano Energy 61 (2019) 428–434, https://doi.org/10.1016/j.nanoen.2019.05.003.
[62] Q. Cui, G. Qin, W. Wang, K.R. Geethalakshmi, A. Du, Q. Sun, Novel two-dimensional MOF as a promising single-atom electrocatalyst for CO_2 reduction: A theoretical study, Appl. Surf. Sci. 500 (2020) 143993, https://doi.org/10.1016/j.apsusc.2019.143993.
[63] E. Shustorovich, Chemisorption phenomena: Analytic modeling based on perturbation theory and bond-order conservation, Surf. Sci. Rep. 6 (1986) 1–63, https://doi.org/10.1016/0167-5729(86)90003-8.
[64] E. Shustorovich, A.T. Bell, Analysis of CO hydrogenation pathways using the bond-order-conservation method, J. Catal. 113 (1988) 341–352, https://doi.org/10.1016/0021-9517(88)90263-1.
[65] C. Di Valentin, G. Pacchioni, M. Bernasconi, Ab Initio Molecular Dynamics Simulation of NO Reactivity on the CaO(001) Surface, J. Phys. Chem. B 10 (2006) 8357–8362, https://doi.org/10.1021/jp060815f.
[66] M. Ghoussoub, S. Yadav, K.K. Ghuman, G.A. Ozin, C.V. Singh, Metadynamics-Biased ab Initio Molecular Dynamics Study of Heterogeneous CO_2 Reduction via Surface Frustrated Lewis Pairs, ACS Catal. 6 (2016) 7109–7117, https://doi.org/10.1021/acscatal.6b01545.
[67] S.I. Allec, M. Nguyen, R. Rousseau, V. Glezakou, The role of sub-surface hydrogen on CO_2 reduction and dynamics on Ni(110): An ab initio molecular dynamics study, J. Chem. Phys. 155 (2021) 044702, https://doi.org/10.1063/5.0048894.
[68] K. Schwarz, R. Sundararaman, The electrochemical interface in first-principles calculations, Surf. Sci. Rep. 75 (2020) 100492, https://doi.org/10.1016/j.surfrep.2020.100492.
[69] R. Sundararaman, K. Schwarz, Evaluating continuum solvation models for the electrode-electrolyte interface: Challenges and strategies for improvement, J. Chem. Phys. 146 (2017) 084111, https://doi.org/10.1063/1.4976971.
[70] F. Nattino, M. Truscott, N. Marzari, O. Andreussi, Continuum models of the electrochemical diffuse layer in electronic-structure calculations, J. Chem. Phys. 150 (2019), https://doi.org/10.1063/1.5054588.
[71] J. Tomasi, B. Mennucci, R. Cammi, Quantum mechanical continuum solvation models, Chem. Rev. 105 (2005) 2999–3093, https://doi.org/10.1021/cr9904009.
[72] J. Tomasi, M. Persico, Molecular interactions in solution: An overview of methods based on continuous distributions of the solvent, Chem. Rev. 94 (1994) 2027–2094, https://doi.org/10.1021/cr00031a013.
[73] S. Sakong, M. Naderian, K. Mathew, R.G. Hennig, A. Groß, Density functional theory study of the electrochemical interface between a Pt electrode and an aqueous electrolyte using an implicit solvent method, The J. Chem. Phys. 142 (2015) 234107, https://doi.org/10.1063/1.4922615.
[74] S.P. Liu, M.Z. Yong, F. Zhu, W. Gao, Q. Jiang, Electroreduction of CO_2 to formic acid on Cu: Role of water bilayer in modeling electrochemical interface, Appl. Catal. A Gen. 547 (2017) 214–218, https://doi.org/10.1016/j.apcata.2017.09.002.
[75] J. Liu, Y. Wang, Theoretical identification and understanding of catalytic active sites for water splitting reactions, Catalysis 34 (2022) 1–16, https://doi.org/10.1039/9781839165962-00001.
[76] A.R. Milosavljević, V.J. Cerovski, F. Canon, L. Nahon, A. Giuliani,, Nanosolvation-Induced Stabilization of a Protonated Peptide Dimer Isolated in the Gas Phase, Angew. Chem. Int. Ed. 52 (2013) 7286–7290, https://doi.org/10.1002/anie.201301667.
[77] F. Calle-Vallejo, R.F. de Morais, F. Illas, D. Loffreda, P. Sautet, Affordable Estimation of Solvation Contributions to the Adsorption Energies of Oxygenates on Metal Nanoparticles, J. Phys. Chem. C 123 (2019) 5578–5582, https://doi.org/10.1021/acs.jpcc.9b01211.
[78] G. Liberto, F. Maleki, G. Pacchioni, pH Dependence of MgO, TiO_2, and γ-Al_2O_3 Surface Chemistry from First Principles, J. Phys. Chem. C 126 (24) (2022) 10216–10223, https://doi.org/10.1021/acs.jpcc.2c02289.
[79] F. Maleki, G. Di Liberto, G. Pacchioni, pH- and Facet-Dependent Surface Chemistry of TiO_2 in Aqueous Environment from First Principles, ACS Appl. Mater. Interfaces 15 (8) (2023) 11216–11224, https://doi.org/10.1021/acsami.2c19273.
[80] P. Gono, F. Ambrosio, A. Pasquarello, Effect of the Solvent on the Oxygen Evolution Reaction at the TiO_2–Water Interface, J. Phys. Chem. C 123 (30) (2019) 18467–18474, https://doi.org/10.1021/acs.jpcc.9b05015.
[81] G. Di Liberto, S. Tosoni, L.A. Cipriano, G. Pacchioni, A Few Questions about Single-Atom Catalysts: When Modeling Helps, Acc. Mater. Res. 3 (2022) 986–995, https://doi.org/10.1021/accountsmr.2c00118.